CHAPTER IV

RESULTS AND DISCUSSION

Investigation on deposition of ZnO in polyelectrolyte (PET) film on glass substrates was divided into 2 steps, which were preparation of PET film on glass substrate and deposition ZnO in PET films by 3 different methods. The preparation of PET film by the dip coating technique was examined for the suitable conditions to fabricate stable film with smooth surface. Polymer concentration, withdrawal speed (WS) and number of dipping cycle was considered. Stable PET film was subjected to ZnO by the 3 different methods, namely precipitation method, suspension of ZnO in PAA, and sol-gel ZnO method for comparison of the most suitable alternative.

Part A: Effect of polymer concentration, withdrawal speed (WS), and number of dipping cycle

The fabrication of thickness behavior of weak polyelectrolyte was studied by Shiratori and Rubner [42]. They discussed about the effect of pH of polymer solution on thickness of polyelectrolyte film. The incremental thickness relates to the individual polycation (PAH) and polyanion (PAA) layers and highly sensitive to pH of dipping solution. Either an increase or a decrease in charge density of polyelectrolyte could affect the polycation or polyanion film thickness in a range of 5 to 80 Å regarding to the control of the pH of polyelectrolyte solution. For that reason, in this work, pH of polyelectrolyte solution was adjusted using 1.0 M HCl in order to control of charge density on each coating layer. pH of PAH and PAA was adjusted to find out a suitable condition to fabricate a bilayer PET film. Based on our preliminary experiments PAH layer was prepared in prior to dipping into PAH solution at pH 1.5 which could provide a stable bilayer film on glass substrate.

4.1 Effect of polymer concentration

Preparation of PET film was prepared using various concentration of PAH and PAA with the aim of investigation effect of polymer concentration on film characteristics. Both of PAH and PAA concentration was in the range of 0.02 to 2.00M. Confocal laser scanning microscope (CLSM) was employed to characterize thickness of fabricated film after drying operation at the temperature of 180°C. The films produced from various polymer concentrations show a considerable difference in the thickness as shown in Figure 4.1. The film thickness, represented by root mean square (RMS), was estimated to be 1.701, 1.916, 2.364, 2.698, and 2.897 μm for 0.02, 0.20, 0.50, 1.00, and 2.00 M, respectively. This indicates a strong influence of the polymer concentration on the film thickness because a higher concentration of polymer solution could provide the higher film thickness. It can be concluded that 2.0 M PAH/PAA at a constant withdrawal speed (WS) of 3 cm/min is suitable for fabricating PET film.

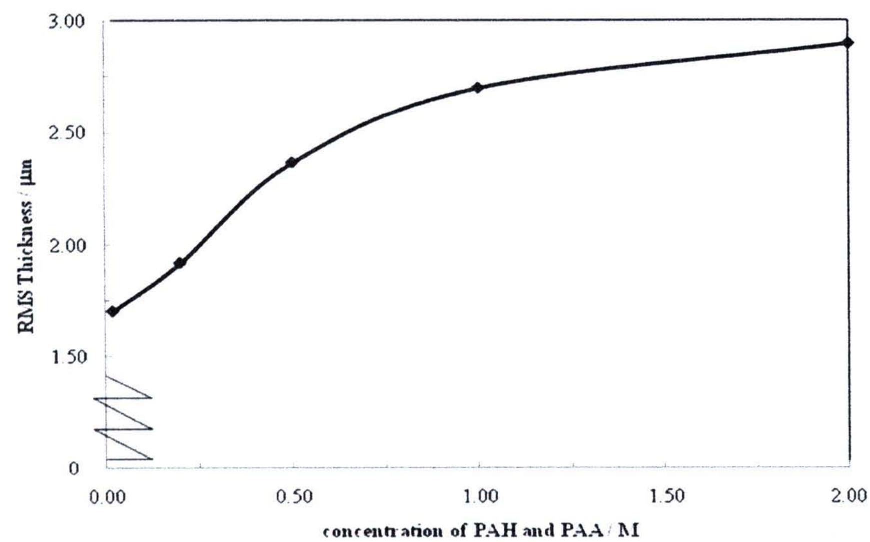

Figure 4.1 Film thicknesses as a function of polymer concentration of PAH and PAA in a range of 0.02-2.00 M

It would be noted that, the solution concentration is also related to the solution viscosity. The viscosity of PAH and PAA was characterized by a rheometer at room temperature. The incremental viscosity of the polymer solution depends on the increased polymer concentration as summarized in Table 4.1. The incremental film thickness as the solution concentration was increased; would be described to the increased amount of liquid attracting on the dipped glass substrate. The thickness dependency on the solution viscosity was also reported by Yimsiri and Mackley [35]. They discussed experimental observation on spin and dip coating of light-emitting polymer (LEP) solution. It was found that film thickness was essential dependent on the combined effect of viscosity and concentration. The amount of the liquid moving upwards with the substrate at the same withdrawal speed is larger for a more viscous liquid due to the drag force (ηu_0) is proportional to the effect of solution viscosity on the film thickness where η is a polymer solution viscosity and u_0 is the solvent evaporation rate.

Table 4.1 Viscosity of PAH and PAA at different concentration

Concentration of PAH (M)	Viscosity (cP)
0.02	1.16
0.20	3.71
0.50	10.57
1.00	10.93
2.00	35.23

Concentration of PAA (M)	Viscosity (cP)
0.02	0.95
0.20	1.18
0.50	1.80
1.00	1.90
2.00	11.33

In term of optical property, a transparent film prepared from polymer concentration in a range of 0.02-2.0 M was examined by UV-VIS in the wavelength of 300-800 nm as shown in Table 4.2. It was found that the average transmittances of the various polymer concentrations coated on glass substrates that prepared by WS 3 cm/min and dried temperature of 180 degree are higher than 95 %. However, the optical transmittances slightly decreased while the concentration increased.

Table 4.2 Summary of optical transmittance of PET film prepared with different concentration of PAH/PAA at withdrawal speed of 3.0 cm/min and dried temperature at 180°C

PAH/PAA concentration (M)	Average transmittance (%) (300-800 nm) (Ref. = glass)
0.02	99.9
0.20	99.6
0.50	98.8
1.00	98.9
2.00	95.8

4.2 Effect of withdrawal speed

From the previous experiment, it was found that the polymer concentrations insignificantly effect on the film transparency then, the withdrawal speed of dip coater was further investigated to expose whatever it was possible to improve the thin film transparency. The fabrication of PET films at the polymer concentration of 1.0 M and 2.0 M (as a result shown in the effect of polymer concentration on film thickness) and drying temperature at 180°C were fabricated with a various withdrawal speed in the range of 3.0-9.0 cm/min. Then, the roughness surface of the fabricated film was observed by atomic force microscopic (AFM) as shown in Figure 4.2. It exhibits worm-like appearance.

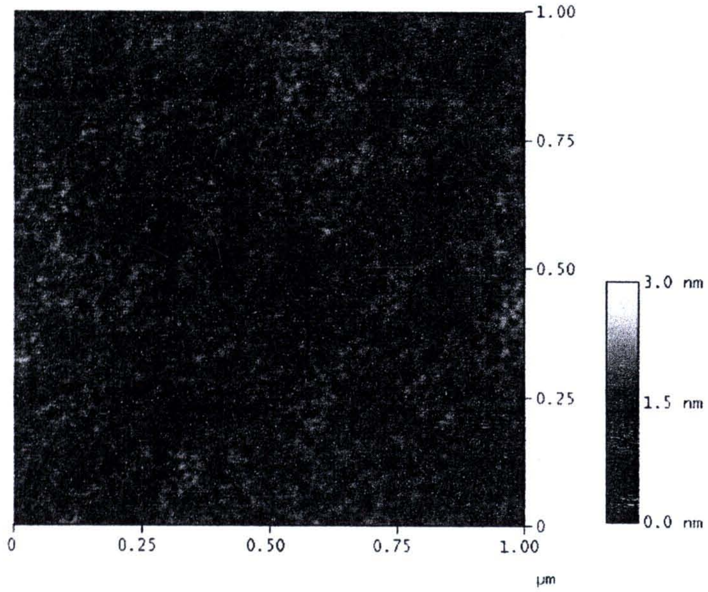

Figure 4.2 AFM topographical image of polyelectrolyte film as prepared by 2.0 M PAH/PAA at withdrawal speed of 3 cm/min and drying temperature of 180°C

Table 4.3 Summary of optical transmittance of PET film prepared with 1.0 and 2.0 M PAH/ PAA coated at different withdrawal speed of 3.0-9.0 cm/min and drying temperature of 180°C

PAH / PAA concentration (M)	Withdrawal speed (WS) (cm/min)	Average transmittance (%) (300-800 nm) (Ref. = glass)
1.00	3.0	99.2
	6.0	97.4
	9.0	96.8
2.00	3.0	92.1
	6.0	91.5
	9.0	90.9

Based on the analytical results of the optical transmittance, the polyelectrolyte film prepared by a higher withdrawal speed has lower transparency as shown in Table 4.3. This is due to the fact that a high withdrawal speed yields a thicker film with opaque appearance. Though, Numpud et al. reported that the optical property of the films prepared from different withdrawal speeds was insignificantly different, the withdrawal speed affected the thickness and surface roughness of films [34]. Based on experimental results of Laudau and Levich, a higher withdrawal speed gives a larger force resulting in great amount of liquid moving upwards toward the substrate surface and a thicker film is obtained [43]. The relation between film thickness and withdrawal speed can be described as a function of withdrawal speed (*h*), solvent evaporation rate (u_0), $h \propto u_0^x$ (*x* as the exponent obtained from the experiment). Therefore, film thickness and surface roughness of the polyelectrolyte film at different withdrawal speed was determined by CLSM at the magnification of 20X.

Table 4.4 Film thickness and RMS roughness of PET films determined by CLSM

PAH and PAA concentration (M)	Withdrawal speed (WS) (cm/min)	Film thickness (μm)	RMS roughness (μm)
1.0	3	2.46	0.03
	6	2.46	0.04
	9	2.98	0.07
2.0	3	3.60	0.03
	6	3.64	0.04
	9	3.67	0.06

From the data in Table 4.4, the films prepared from 1.0 M and 2.0 M show the thickness ranging from 2.46-3.67 μm. And, the RMS roughness of the film prepared from both concentrations as the withdrawal speed was increased. This trend corresponds to the CLSM image show in Figure 4.3. It was found that the apparent film shows high surface roughness since the increased withdrawal speed. From this result, it can be concluded that at the same withdrawal speed, the polymer concentration affects only the film thickness but not the RMS roughness.

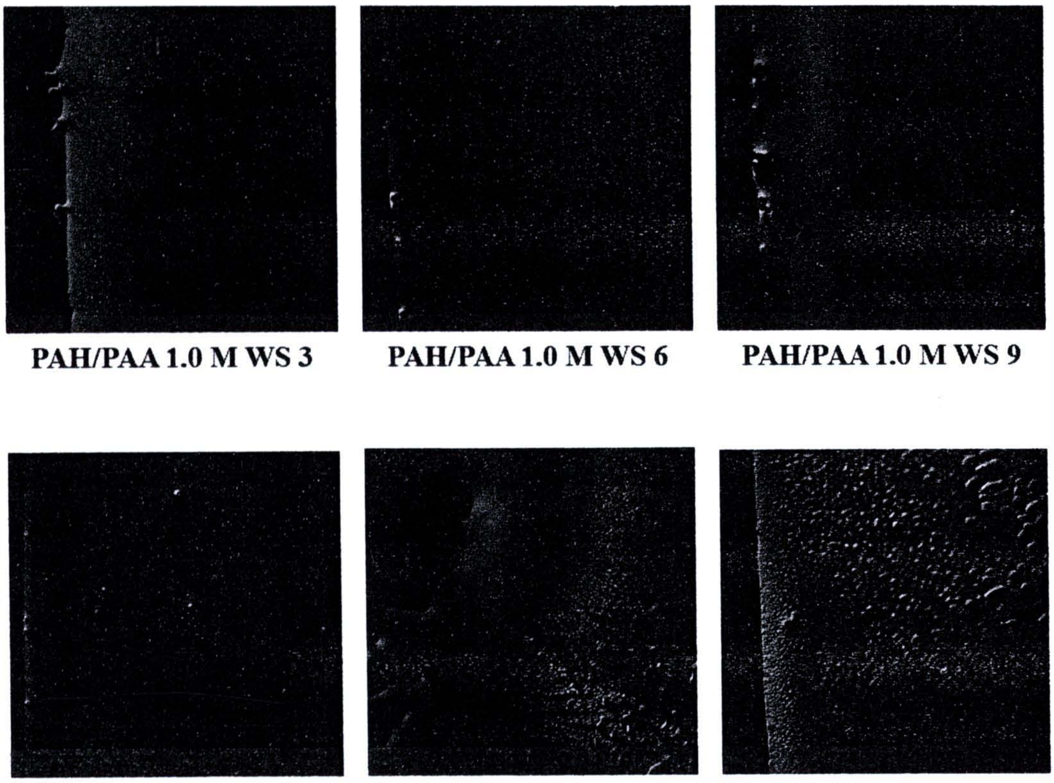

PAH/PAA 1.0 M WS 3 PAH/PAA 1.0 M WS 6 PAH/PAA 1.0 M WS 9

PAH/PAA 2.0 M WS 3 PAH/PAA 2.0 M WS 6 PAH/PAA 2.0 M WS 9

Figure 4.3 Apparent films obtained by confocal laser scanning microscopy (CLSM) observation through polyelectrolyte film on a glass substrate as prepared by different concentration with various withdrawal speeds in a range of 3.0-9.0 cm/min and drying temperature of 180°C

From these results, it was suggested that the film prepared from 2.0 M PAH/PAA with withdrawal speed 3 cm/min gives the proper thickness and fine surface. This concentration and withdrawal speed were chosen for further study affecting the film thickness, surface roughness and film transparency. However, polymer concentration and withdrawal speed of dip coater have exerted slight effects on the thickness and transparency of the film. Many studies have been investigated about the incremental number of dipping cycle influence the thickness and surface roughness of the PET film thickness [3, 44]. Then, the effect of number of layer on the thickness and surface roughness was further investigated.

4.3 Effect of number of dipping cycle on film thickness

Many studies have been investigated on the number of dipping cycles affect the thickness and surface roughness of the PET film thickness [3, 45]. The effect of number of layers on the thickness and surface roughness was investigated in this work. The thickness and surface roughness of polyelectrolyte films coating on glass substrates were analyzed using CLSM. It was found that the single bilayer film prepared by using 2.0 M and WS of 3.0 cm/min exhibited a similar thickness as compared to that of double and triple bilayer films according to the dissolution of the coated film into the dipping solution after repetitive cycles. All number of dipping cycles gives similar surface roughness as evidenced from RMS roughness of 0.03, 0.02 and 0.03 μm for single bilayer, double bilayer and triple bilayers, respectively.

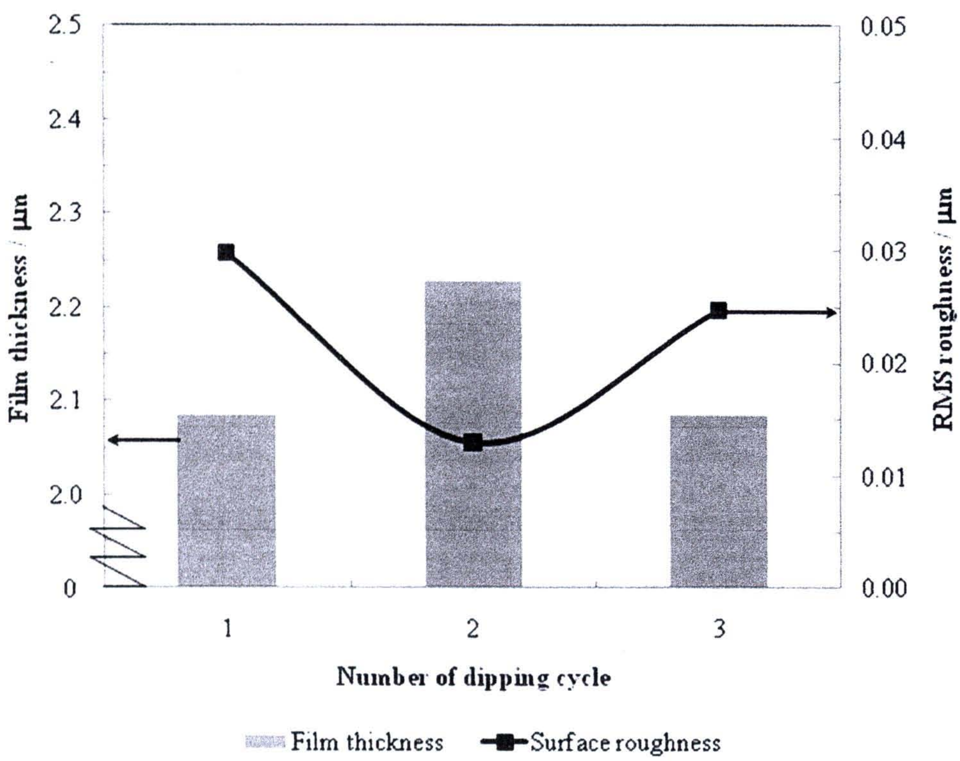

Figure 4.4 A plot of film thickness and surface roughness of PET films vs. number of dipping cycles

Figure 4.4 presents the effect of number of dipping cycle on the film thickness and RMS roughness. The film thickness of single, double, and triple bilayers coating films is 2.086, 2.227, and 2.085 μm, respectively. Interestingly, film thickness is independent to the number of dipping cycles since dipole force between polyelectrolyte film and glass substrate may be lower than viscous force of polymer solution in the step of drainage in the dip coating technique.

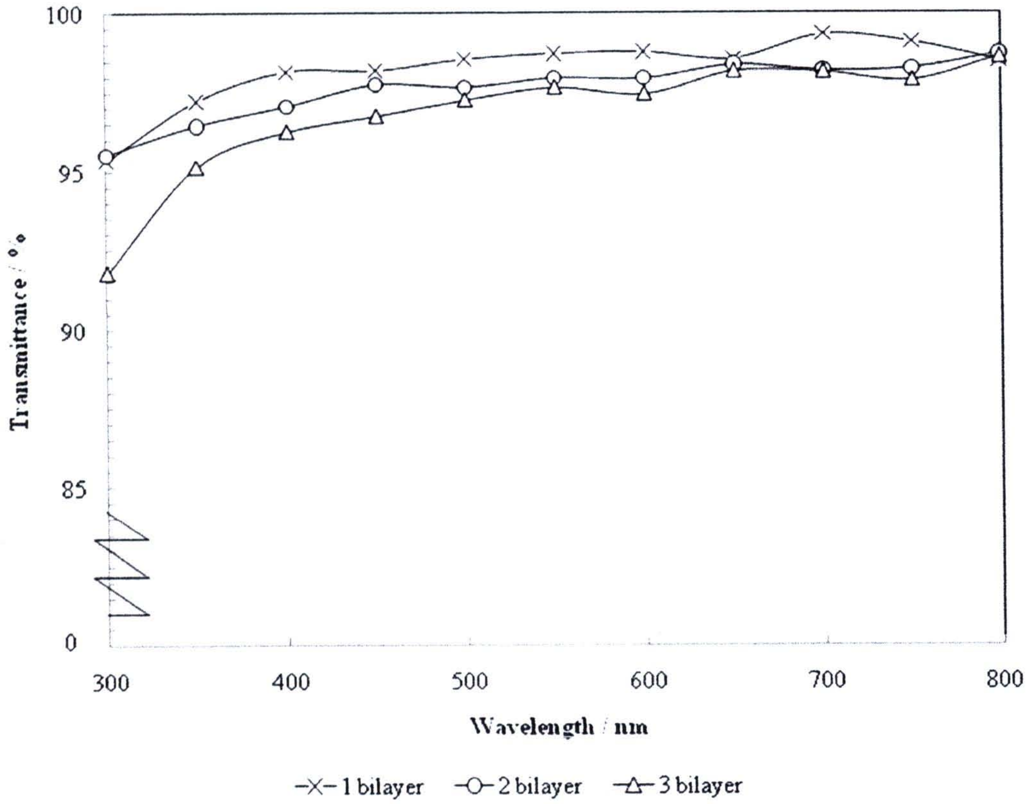

Figure 4.5 Optical transmittance of polyelectrolyte film at different number of dipping cycle such as 1 bilayer, 2 bilayer and 3 bilayer

The optical transmittance spectra of the various polyelectrolyte bilayer films were presented in Figure 4.5. The increased number of dipping cycles hence the lower transmittance of the polyelectrolyte film. These results implied that a single bilayer of polyelectrolyte film prepared by 2.0 M polymer solution with withdrawal speed of 3.0 cm/min was proper for our applications.

Part B: Effect of methodology for depositing ZnO onto the etched PET film

In general, superhydrophilicity of the film surface can be controlled by the surface roughness and surface energy by coating the metal oxides that aids the wetting property of the surface. Among numerous materials, ZnO can be chemically activated by UV light that significantly modified its wettability [7]. ZnO thin film can be deposited by several techniques such as pulsed laser deposition, sputtering, spray pyrolysis, electrodeposition, chemical vapor deposition, molecular beam epitaxy, pulsed laser deposition, metal-organic chemical vapor deposition and sol-gel dip coating technique [9-10, 12, 22, 26, 28, 46-50]. Recently, inorganic semiconductor nanoparticles embedded in polymer matrices have been investigated, since they can be used in optical, electrical, magnetic devices and surface wettability [3, 10, 17]. Moreover, a combination of ZnO and polyelectrolyte film can provide a promising alternative for substrate modification. However the information on the advantages of incorporating ZnO with polyelectrolyte films for a control hydrophilic and hydrophobic property of coated substrates is still limited. Then, ZnO incorporated with polyelectrolyte film was studied by using different method in order to improve transparency and hydrophilicity of the film.

4.4 Precipitation of ZnO into polyelectrolyte film

Wang et al. prepared polymer films by embedding ZnO nanocrystals in multilayer polymer films (PDDA and PSS) using $Zn(NO_3)_2$ and NH_4OH as precursor [9]. It was found that the morphologies of ZnO particles were controlled by a number of precipitation cycles. This approach provides an effective route for construct multilayer film containing ZnO nanoparticles. Modified from Wang et al., film was fabricated by immersing the appropriate polyelectrolyte film from part A into 0.01 M $Zn(NO_3)_2$ solution for 15 min, subsequently dipping into NH_4OH solution (0.01 M) for 30 sec. This process is accounted as one precipitation cycle. The number of cycles was varied in the range of 1 to 5. The time between each cycle is 20 min. All films were dried at 180°C for 2 h.

Table 4.5 Summary of optical transmittance of ZnO thin films prepared with different number of precipitation cycle at withdrawal speed of 3.0cm/min and dried temperature at 180°C

Number of precipitation cycle	Average transmittance (%) (350-800 nm) (Ref. = glass)
1	99.4
2	99.5
3	95.4
4	86.1
5	97.8

Based on the analytical results of optical transmission, it was observed that the number of precipitation cycles could affect the film transparency as shown in Table 4.5. The decrease in transmittance indicates that more particles nucleate in the polyelectrolyte film with increasing precipitation cycles of Zn^{2+}. However, the film was more transparent when the number of precipitation cycle was increased to 5. This is attributed to the fact that at precipitation cycle higher than 4, Zn^{2+} was dissolved by the ammonium hydroxide in the previous layer. Moreover, the formation of tetrahydroxozincate might be increased as the hydroxyl group increased with an increasing number of precipitation cycle up to 5. These effect resulting in the translucency of the prepared film. However, the film with lower transmittance would contain more quantity of ZnO. The film with a precipitation cycle of 3 and 4 contained higher quantity of ZnO and was selected for further studies.

Table 4.6 Film thickness and RMS roughness of ZnO film at different number of precipitation cycle was observed by CLSM

Number of precipitation cycle	Film thickness (μm)	RMS roughness (μm)
1	2.03	0.048
2	2.39	0.058
3	4.27	0.062
4	4.50	0.076
5	4.57	0.080

The effect of precipitation cycles on the film thickness and surface roughness of ZnO thin film on glass substrates is shown in Table 4.6. The thickness of the prepared film slightly changes from 4.50 to 4.57 μm when the precipitation cycle is increased from 4 to 5. This indicated that the precipitation cycle higher than 4 would not provide a great amount of the deposited film on glass substrate. However, the surface roughness of the fabricated film dramatically increases from 0.048 to 0.080 μm as the number of precipitation increase. Regarding to confirm the surface roughness of the film as prepared by number of precipitation cycles of 3 and 4 (selected by a lower transmittance from previous experiment), the film was observed by AFM as shown in Figure 4.6 and 4.7, respectively.

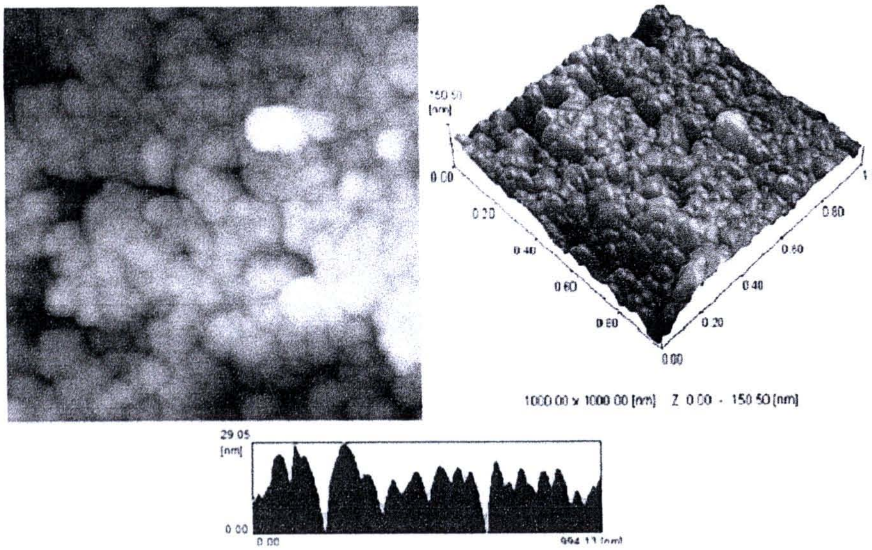

Figure 4.6 2D and 3D topographical (1μm×1μm) of ZnO in PET film prepared by 3 precipitation cycles

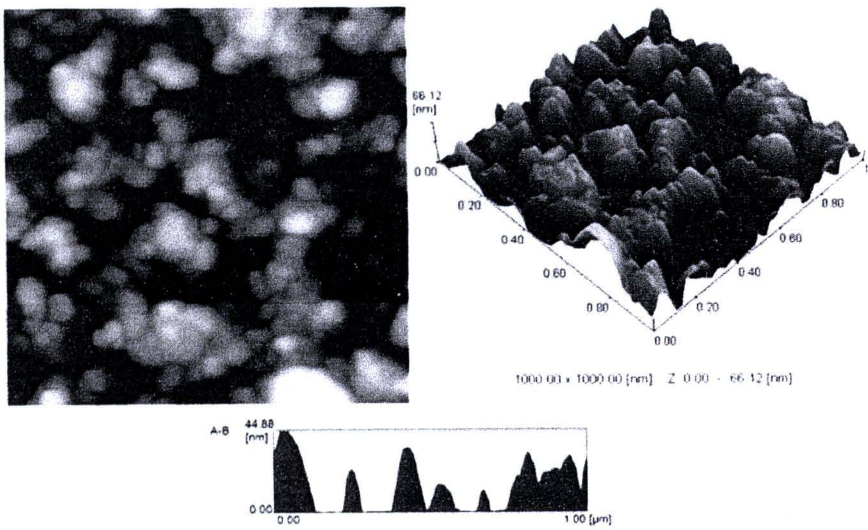

Figure 4.7 2D and 3D topographical (1μm×1μm) of ZnO in PET film prepared by 4 precipitation cycles

It was found that the number of precipitation changing from 3 to 4 cycles resulted in the average grain size increasing from 29.05 to 44.88 nm. The large grain size make possible the agglomeration; leading to high surface roughness. In order to confirm the chemical composition of the fabricated film, energy dispersive X-ray spectroscopic analysis was used for elemental analysis of the prepared films as shown in Figure 4.8.

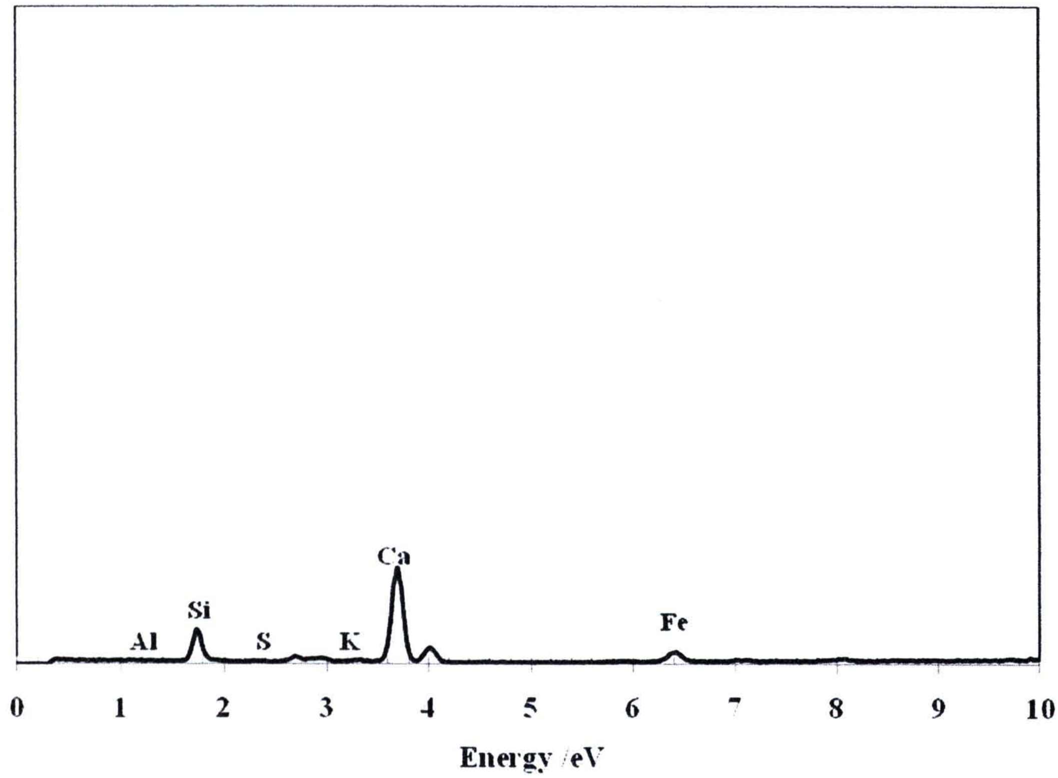

Figure 4.8 EDX analysis of ZnO thin film prepared with 3 precipitation cycles coated at withdrawal speed of 3.0 cm/min and drying temperature at 180°C for 2h

The EDX data of 3 precipitation cycles, ZnO in polyelectrolyte film shows no evidence of Zn, indicating that the film has very low content of Zn. Then, a higher concentration of $Zn(NO_3)_2$ (0.1 M) for precipitation ZnO thin film was used for prepared

ZnO in polyelectrolyte film. It was found that the prepared film exhibits transmittance lower than 60% and showing a peak of Zn in the EDX spectrum as shown in Appendix 1. Additionally, the film crystalline was also analyzed by XRD. The result gave no indication for the characteristic phase of the ZnO as shown in Appendix 3. Therefore, on the basis of EDX and XRD results, it may be concluded that the film was not crystalline and had a very low content of ZnO. As a consequence, there was no further study on the photoinduced hydrophilic properties of the film.

Accordingly, ZnO particles in polyelectrolyte film prepared from precipitation method cannot be obtained by the standard method. Then, we further studied on another method (suspension of ZnO in PAA and sol-gel ZnO) for depositing ZnO in polyelectrolyte film to improve their photoinduced hydrophilic property.

4.5 Suspension of ZnO in PAA

A schematic image of the PET coating film was depicted in Figure 4.9(a). The PAH/PAA coating layers were then subject to a chemical etching process using HCl solutions with pH of 2.3 and 1.1. The increased roughness of a surface can increase its hydrophilicity dramatically and the hydrophobic surface becomes more hydrophobic corresponding to Wenzel state [19, 44].

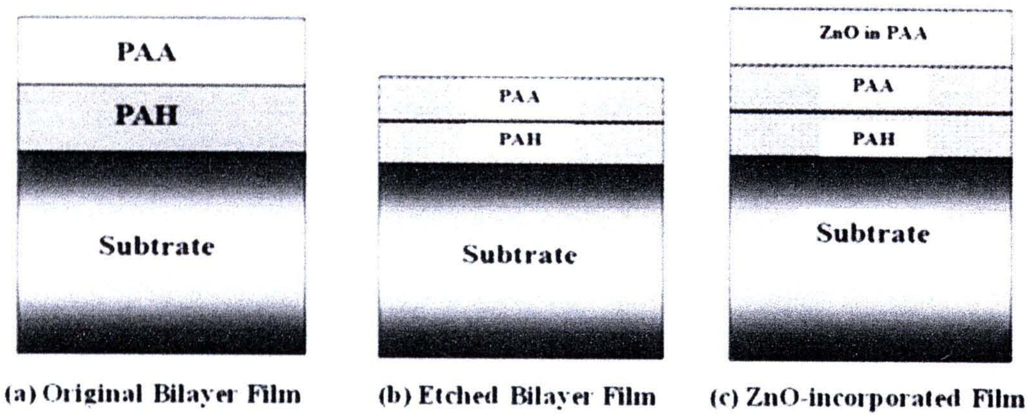

Figure 4.9 Schematic diagram of coating films

Nimitrakoolchai and Supothina studied the deposition of SiO_2 on the etched PAH/PAA (PET) for superhydrophobic films. The desired surface roughness was obtained by acid etching using HCl with pH 2.3 and 1.1 for various immersion times [3]. The results showed that the opposite trend that probably affected the surface chemistry modified after chemical etching. The increased etching time gave the RMS roughness lower than the as-prepared film but the water contact angle was much higher. Therefore, etching time was further investigated to find out whether it was possible improve the hydrophilic property of the surface. Etching time was varied in a range of 15 to 90 min and drying temperature would be set at 180°C for 2 hrs to manipulate the surface roughness of polyelectrolyte film. The modified surface was coated with suspension of ZnO in PAA. The contents of ZnO in the polymer solution was also investigated to study the effect of the quantity of ZnO on its hydrophilic property

4.5.1 Effect of etching time on the hydrophilicity of the PET film

Comparison of surface roughness of the etched PET film against etching time was shown in Figure 4.10. A different degree of surface roughness of PET film strongly depends on etching time. The etched PET films were subjected to water contact angle analysis. The film thickness and surface roughness in each layer was also measured by CLSM.

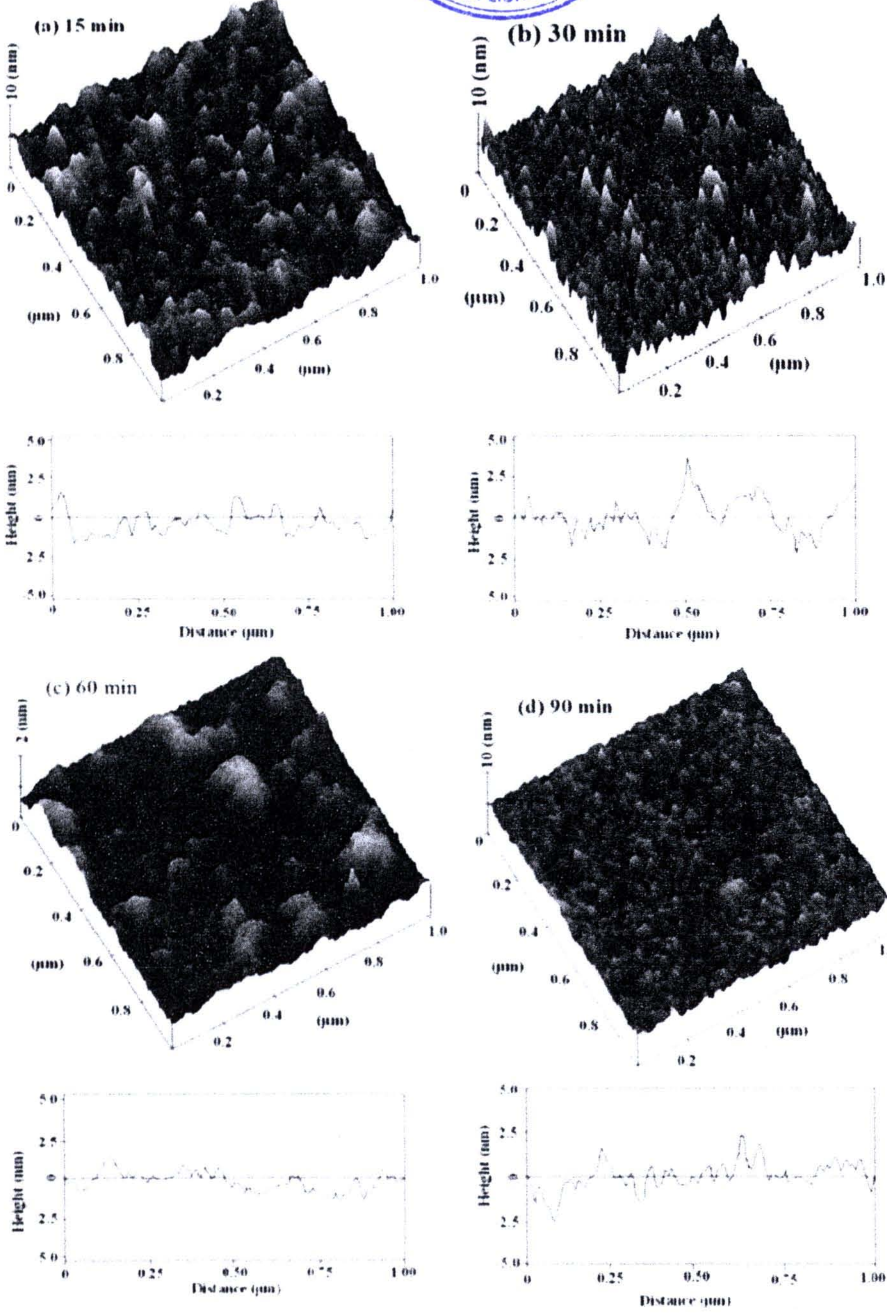

Figure 4.10 2D and 3D topographical images of the PET film etched at different times (a) 15 min, (b) 30 min, (c) 60 min, and (d) 90 min.

Table 4.7 Summary of the water contact angle and surface roughness of each layer

Sample	Contact angle (°)	RMS roughness (nm)
PAH	n/e*	0.714
PAA	69.57	0.187
PAH/PAA (PET)	49.47	0.200
Etch PAH/PAA (PET)_15 min	27.16	1.789
Etch PAH/PAA (PET)_30 min	22.38	1.980
Etch PAH/PAA (PET)_60 min	29.67	1.619
Etch PAH/PAA (PET)_90 min	33.08	0.715

* n/e = not examined according to dissolution of PAH in water

The water contact angle and surface roughness of PAH, PAA, non-etched bilayer PET film and the etched bilyayer PET films were shown in Table 4.7. The bilayer PET film etched for 30 min gave the lowest contact angle and the highest surface roughness. It is clearly shown that the contact angle is decreased when the RMS roughness is increased. This is attributed to the fact that the surface with higher roughness can accommodate the spreading water better. The existence of deeper grooves on the surface with higher roughness will try lower volume of air leading to a better water spreading process and lower water contact angle [46].

4.5.2 Investigation of the ZnO-incorporated PET films

ZnO incorporated with PET film was prepared by immersing the etched PET film into a ZnO suspension in PAA for 15 min (purpose: deposition of ZnO onto the base electrolytic film) which was schematically shown in Fig. 4.9(b). The PAA solution was selected for ZnO suspension due to its stability. PAH cannot be employed for delivering ZnO onto the coated surface because it rapidly dissolves in water. Distribution of ZnO on the PET film was observed by FESEM in the function of COMPO mode and SEI mode as shown in Figure 4.11. The COMPO mode used the back-scattered electrons; a reflection from the sample by elastic scattering [40]. The intensity of back-scattered electrons signal strongly relates to the atomic number (Z) of the specimen. Then, COMPO images provide information about the distribution of different elements in the sample. The element with higher atomic number emits brighter light from Figure 4.11 (b) and (c), the brighter particles shown on the surface are supported to be ZnO. In addition the sizes of ZnO particles as shown in Figure 4.11 (b) and (c) are longer than the ZnO particle used for preparing the film. This may be due to the agglomeration of ZnO particle in PAA.

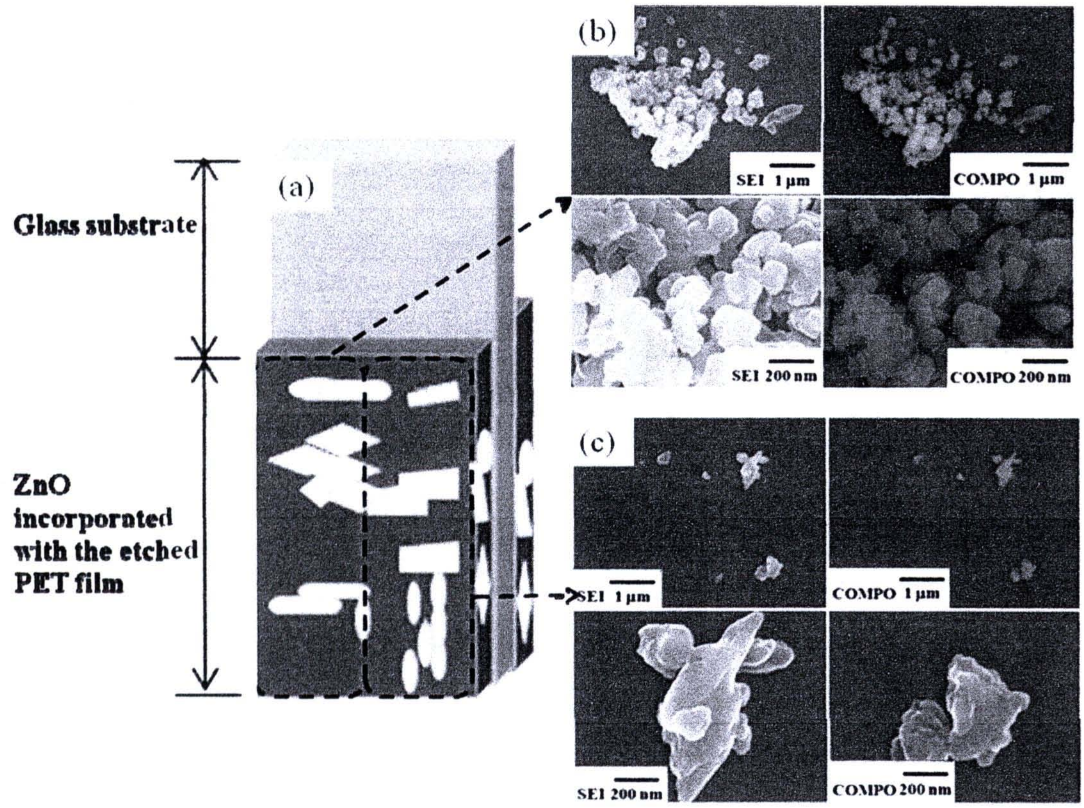

Figure 4.11 (a) Schematic diagram of ZnO distribution on PET film; (b) and (c) FESEM images in SEI and COMPO modes of the ZnO incorporated PET film for the left and right side of the film

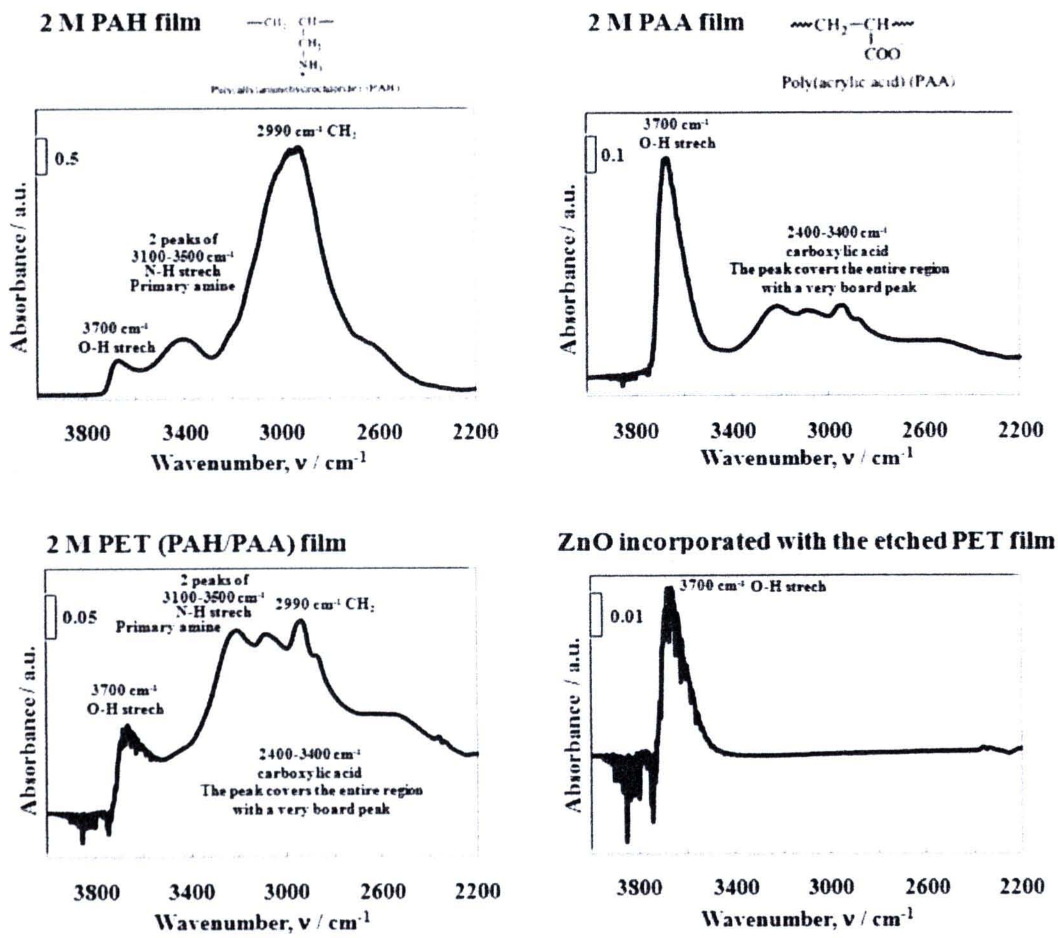

Figure 4.12 FTIR spectra of PAH film, PAA film, PAH/PAA (PET) film and ZnO incorporated with PET film; dried at temperature of 180°C for 2 h.

Figure 4.12 shows infrared spectra of PAH and PAA films deposited onto the glass substrate. The top spectrum was obtained from the film fabricated with a PAH and PAA dipping solution of pH of 1.0 and drying operation at 180°C for 2 h. Wherein, the bottom spectrum was obtained the polyelectrolyte film (PAH/PAA, PET) and the fabricated film with ZnO in PAA deposited onto the PET film which was dried at the same process of PAH and PAA film. The O-H stretch in both of PAH and PAA film had on absorption band of 3700 cm^{-1} [45]. Hence, the water was used as solvent to prepare polymer solution although the films were dried. The films would have a little water content.

The PAH film exhibits the peak of CH_2 at the absorption band of 2990 cm^{-1}. It was observed that the two peaks of N-H stretch of primary amine about 3100-3500 cm^{-1}. The results corresponded to structural of PAH as well as in the same case of PAA. The peak of interest in the spectra of PAA is carboxylic acid at 2400-3400 cm^{-1}. This peak always covers the entire region with a very broad peak. The alternate functional group of PAA deposited on PAH film was reaction between PAH and PAA film (investigated by FTIR). It is clearly represented the PAH bond with PAA since the absorption bands of PAH near 2990 cm^{-1} (CH_2) and the two peaks of 3100-3500 cm^{-1} (primary amine) merge with the carboxylic acid absorption band of PAA. In addition, the peak intensity of carboxylic acid was increased when the ZnO was added into the suspension of ZnO in PAA. The ZnO deposited on the etched PET was studied the changeable functional group on the surface. Results showed that the absorption band of PAH and PAA was removed, but the O-H stretch band arising. Then, the ZnO would bond with the etched PET film so the larger particle of ZnO (observed by FESEM). This occurs when the polymer covers the ZnO powder that corresponding to result in size distribution as obtained by Zeta-sizer.

Comparison the particle size distributions of ZnO particle in PAA solution at different concentration showed in Figure 4.13 and 4.14. It was found that the precursor solution of 0.1 wt% ZnO in PAA for fabricating ZnO thin film showed size distribution about 5.6 μm. It was larger than the size distribution of 0.2 wt% ZnO in PAA. This evidence confirms that ZnO will bond with water in polymer aqueous solution after mixing between ZnO and PAA solution. Therefore, high content of water in the polymer solution should provide a greater size of ZnO.

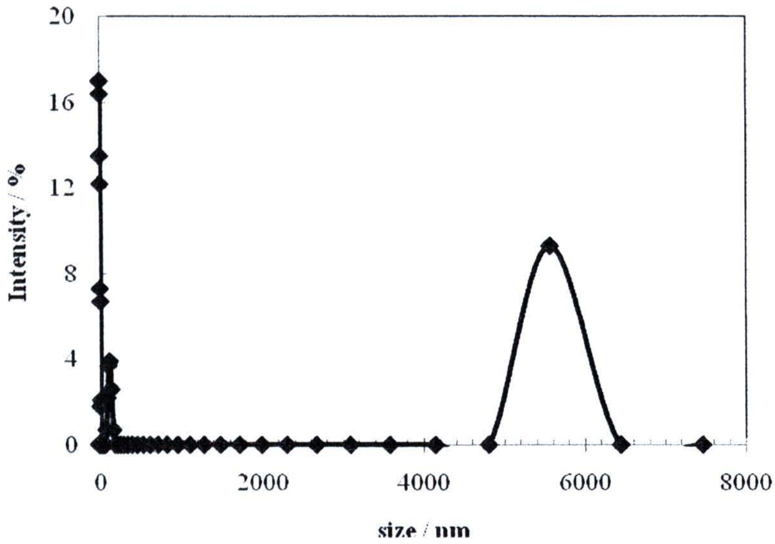

Figure 4.13 Particle size distribution of ZnO in poly(acrylic acid) (PAA) solution at concentration of 0.1 wt % ZnO in PAA for depositing ZnO into etched polyelectrolyte film

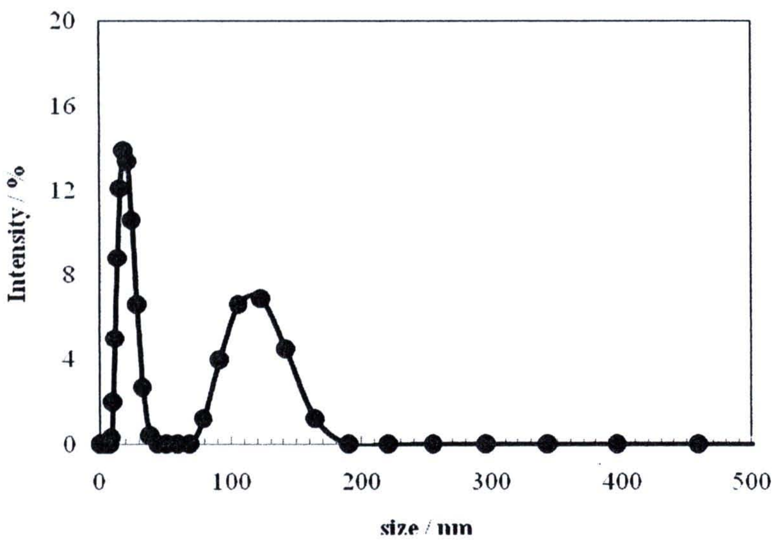

Figure 4.14 Particle size distribution of ZnO in poly(acrylic acid) (PAA) solution at concentration of 0.2 wt % ZnO in PAA for depositing ZnO into etched polyelectrolyte film

Based on the water contact angle, the hydrophilicity of ZnO/PAA films were significantly improved after the UV irradiation of 0 to 60 min as shown in Figure 4.15. Before irradiation, the coating film prepared from 0.2 wt% ZnO suspension exhibited a contact angle of 36.91 degree. The contact angle significantly decreased to 13.74 and 11.11 degree after irradiation time was increased from 1800 and 3600 sec. In addition, it was found that the water contact angle of the coating film prepared from 0.2%wt ZnO suspension was lower than that of film prepared from 0.1 wt% ZnO suspension. In addition, the contact angle of ZnO/PAA film is significantly lower than that of original PET film due to the photosensitive behavior of ZnO that (semiconductor) with band gap energy of ~3.37 eV [51]. The UV illumination onto ZnO nanoparticles enhanced water adsorption on their surface according to the photo-generated surface defective site.

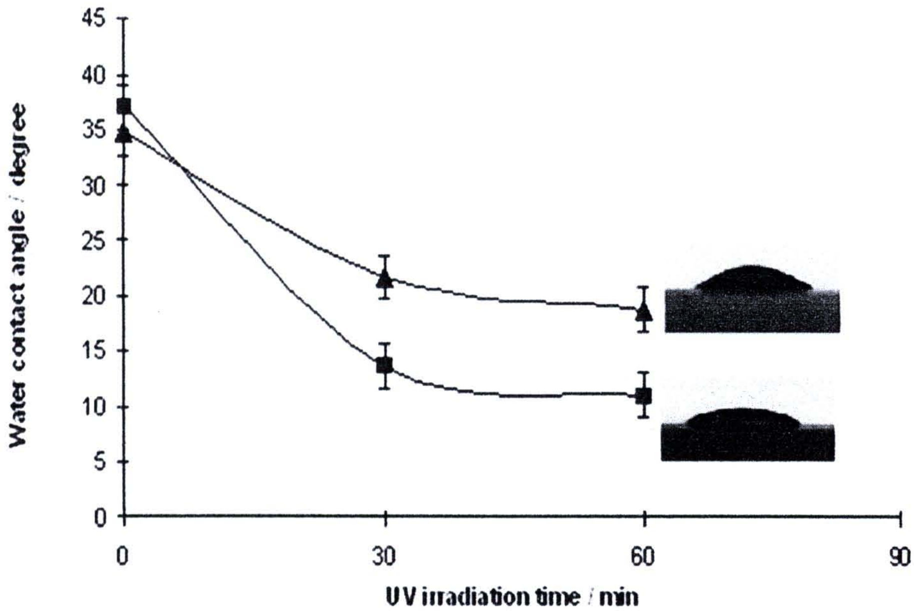

Figure 4.15 Water contact angle vs UV irradiation time of ZnO in PAA on etched PET film (▲ = 0.1 wt% ZnO in PAA on etched PET film, ■ = 0.2 wt% ZnO in PAA on etched PET film)

Such difference in the content of ZnO in suspension provided a hint in their constituent difference. Therefore, energy dispersive X-ray spectroscopic analysis has been achieved for elemental analysis of the coated film as shown in Figures 4.16-4.20.

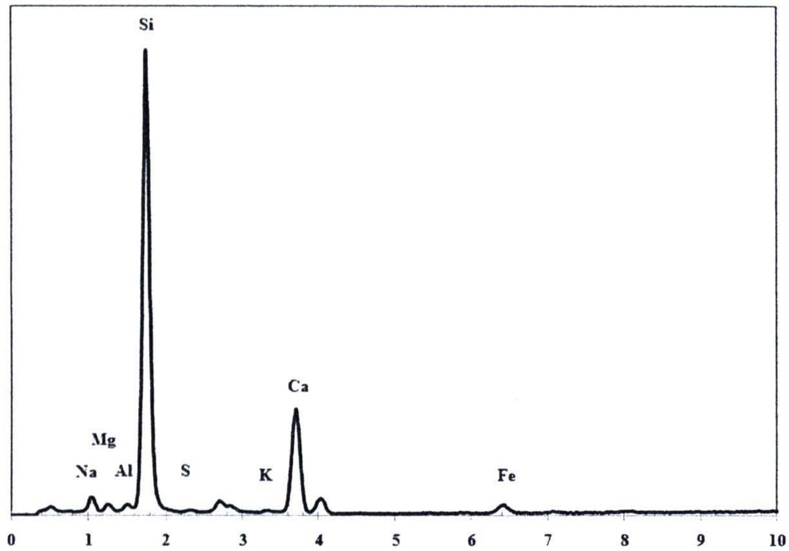

Figure 4.16 EDX analysis of glass substrate

Table 4.8 Summary of the oxide compounds on glass substrate observed by EDX

Oxide compound	Weight percent
Na_2O	13.81
MgO	3.75
Al_2O_3	2.28
SiO_2	72.61
SO_3	0.31
K_2O	0.20
CaO	6.94
Fe_2O_3	0.10

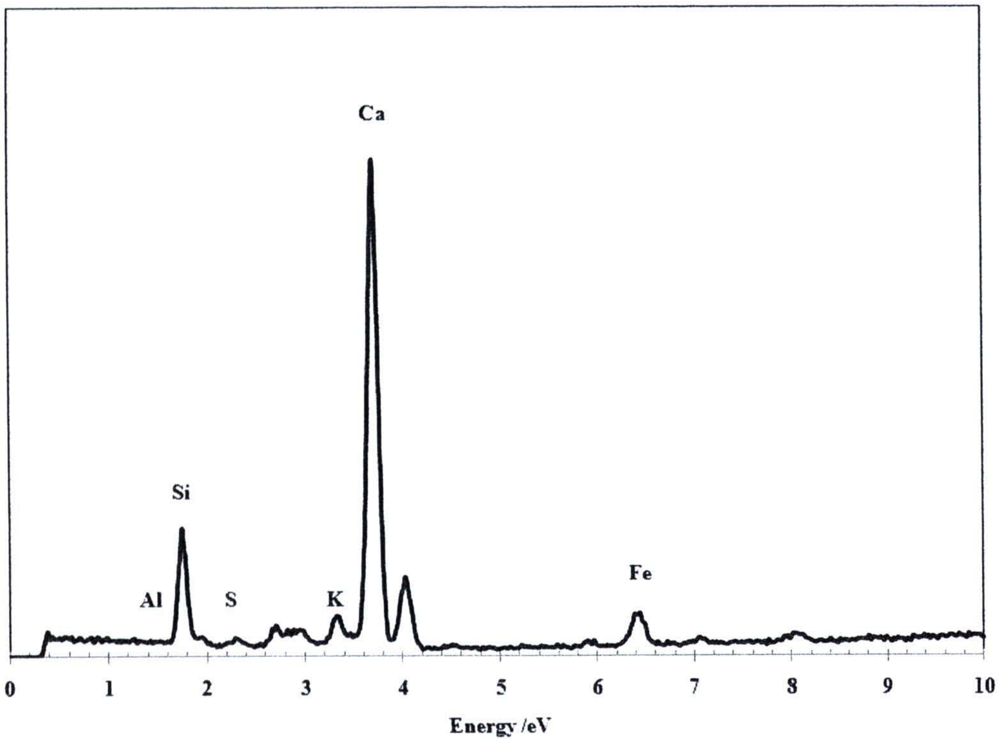

Figure 4.17 EDX analysis of polyelectrolyte film prepared with PAH/PAA concentration of 2.0 M coated at withdrawal speed of 3.0 cm/min and drying temperature at 180°C for 2 h

Table 4.9 Summary of the oxide compounds on polyelectrolyte film observed by EDX

Oxide compound	Weight percent
Al_2O_3	3.30
SiO_2	80.70
SO_3	1.27
K_2O	1.31
CaO	13.26
Fe_2O_3	0.16

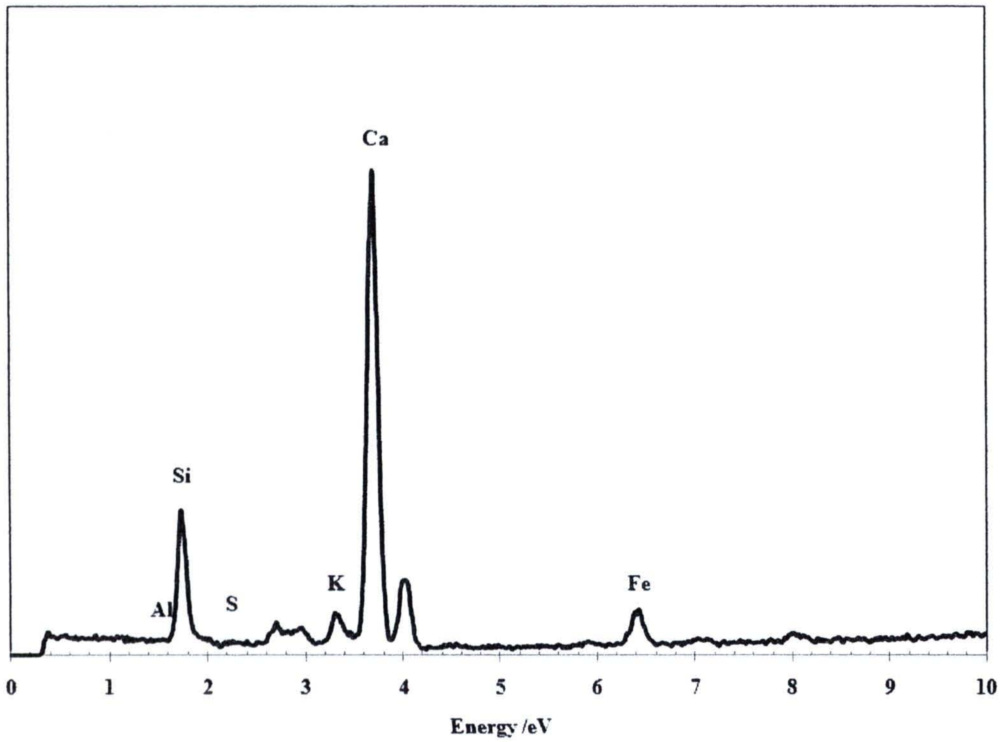

Figure 4.18 EDX analysis of an etched polyelectrolyte film for 30 min and drying temperature of 180°C for 2 h

Table 4.10 Summary of the oxide compounds on the etched polyelectrolyte film for 30 min observed by EDX

Oxide compound	Weight percent
Al_2O_3	2.73
SiO_2	83.98
SO_3	0.26
K_2O	1.16
CaO	11.87

A typical EDX spectrum as shown in Figure 4.7 exhibits that the PET (PAH/PAA) film coated on glass substrate using PAH/PAA concentration of 2.0 M with withdrawal speed of 3.0 cm/min and drying at 180°C was composed of Al, Si, S, K, Ca and Fe. Meanwhile, EDX spectrum of the glass substrate as shown in Figure 4.14 consisted of Na, Mg, Al, Si, S, K, Ca and Fe. It is clearly observed that the coated PET film may prevent diffusion of Na^{+} and Mg^{+} from glass to the surface since the dried substrate at the high temperature. Moreover, the EDX spectrum of the etched PET film still shows the element of Al, Si, S, K and Ca as well as the result of PET film. Consequently, compound oxide in the each layer that observed by EDX, it can be calculated that shown in the Table 4.8-4.10.

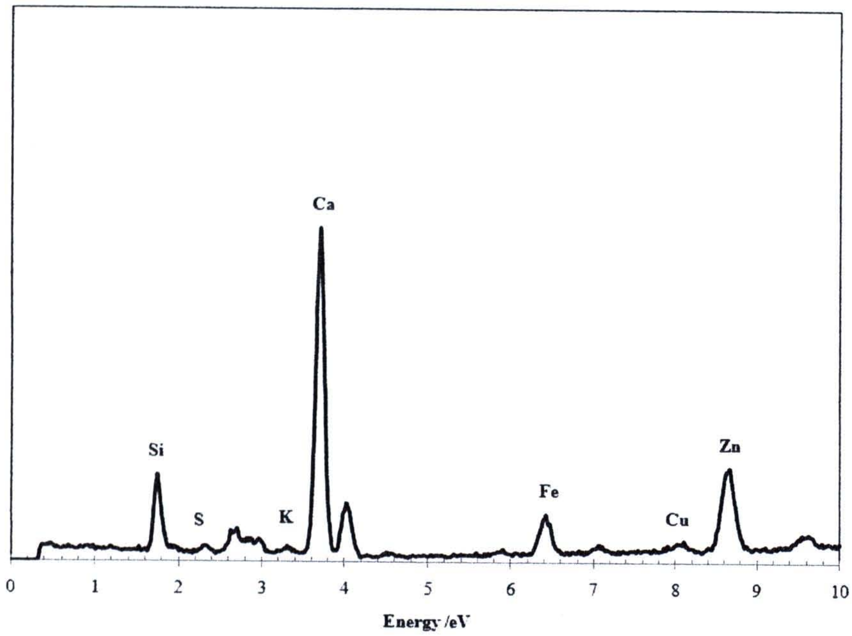

Figure 4.19 EDX analysis of ZnO film prepared by dipping the etched polyelectrolyte film in 0.1 wt% ZnO in PAA solution for 15 min and drying temperature of 180°C for 2 h

Table 4.11 Summary of the oxide compounds on the ZnO film (prepared by dipping the etched polyelectrolyte film in 0.1 wt% ZnO in PAA solution) observed by EDX

Oxide compound	Weight percent
SiO_2	82.82
SO_3	2.14
K_2O	0.39
CaO	14.10
Fe_2O_3	0.30
CuO	0.03
ZnO	0.22

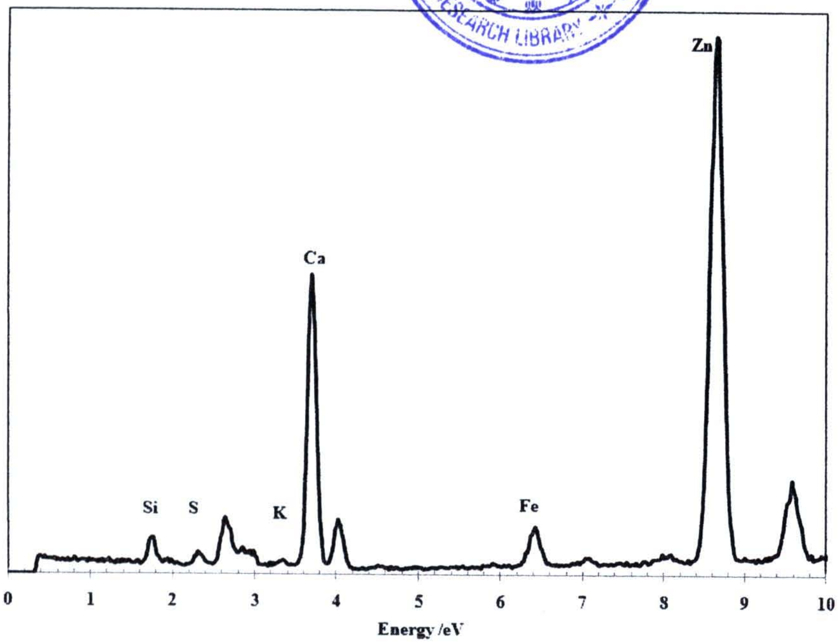

Figure 4.20 EDX analysis of ZnO film prepared by dipping the etched polyelectrolyte film in 0.2 wt% ZnO in PAA solution for 15 min and drying temperature of 180°C for 2 h

Table 4.12 Summary of the oxide compounds on the ZnO film (prepared by dipping the etched polyelectrolyte film in 0.2 wt% ZnO in PAA solution) observed by EDX

Oxide compound	Weight percent
SiO_2	62.10
SO_3	7.09
K_2O	0.61
CaO	25.80
Fe_2O_3	0.70
ZnO	3.70

Comparison of the Figure 4.19 and 4.20 as shown the EDX analysis of ZnO film were prepared by varying the content of ZnO in PAA from 0.1 to 0.2 wt% and both specimens were also dried at 180°C for 2 h. It was found that with the 0.2 wt% ZnO in PAA the highest Zn was obtained. Consequently, the oxide compound film prepared by 0.1 and 0.2 wt% ZnO in PAA show different quantity of ZnO in their layer which exhibit in Table 4.11 and 4.12, respectively. This is evidence to confirm that the higher concentration of ZnO in PAA provides a higher possibility of ZnO deposition within the coating PAA film. Moreover, the ZnO film was also obtained the phase of ZnO in the film by XRD which shown in the appendix B2-B3. However, this characterization may not be suitable for observing the low content of ZnO on the coated film in this experiment because it cannot found the peaks at 31.72°, 34.4° and 36.2° within the X-ray diffratograms assigns to the (100), (002) and (101) planes of ZnO [8].

Regarding to this experimental results, the ZnO suspension in PAA can provide ZnO incorporated with polyelectrolyte films that can improve their hydrophilic property after UV illumination. Nevertheless, this method may occur the agglomeration of ZnO in polymer solution as a result in a larger size of ZnO so it would be irradiated by UV light for long time to be a superhydrophilic surface. Thus, we were also selected as another alternative method for decreasing the irradiation time to progress the hydrophilic property of ZnO thin film.

4.6 ZnO embedded in PET film by sol-gel dip coating method

Currently, the various semiconductors, metallic and magnetic nanoparticles have studied incorporated with polyelectrolyte multilayer films [10]. This method produces by construction the polyelectrolyte (PET) film via the interaction between polycation and polyanion in order to form nanoreactor. Then, the nucleation of metal ion in precursor adsorb into the cavities of the polymers. Most recently, the ZnO nanocrystals were embedded in multilayers polymer films (PDDA and PSS) by using Zn $(NO_3)_2$ and NH_4OH as a precursor. It was found that the morphologies of ZnO particles were controlled by the nucleation and growth from precipitation of reaction cycles. This approach provides an effective route to construct multilayer film containing ZnO nanoparticles. Most results about effects of ZnO sol concentration, ZnO sol aging time and annealing treatment on ZnO thin films have been reported but the effect of pH of ZnO sol on the optical property and hydrophilic property of ZnO thin films is seldom studied. Then, the method of ZnO embedded in PET film by sol-gel dip coating method was investigated the effect of pH of precursor sol on the optical property and morphology of the ZnO before analyzing the hydrophilic property of the film.

4.6.1 Effect of pH of sol on the optical property and morphology of the ZnO embedded in PET film

The ZnO embedded in PET film was observed (the film thickness and surface roughness) by CLSM at the magnification of 20X. It was found that an increased pH the precursor ZnO sol gave thicker film because a large amount of ZnO adsorbed in the cavities of PET film. Then, excess ZnO particle cannot be penetrated into the hole of the polymer, hence may occur (growth grain size on the coated surface) as agglomerate to be a larger size then it exhibits thicker film as shown in Figure 4.21. In addition, the several quantity of ZnO particle on the film was quantitatively correlated with the solvent evaporation, the higher thickness film affects the drying of the solvent. This result was supported by research work of Brinker et al.. Wherein, thicker film gave a longer time to dry the solvent, this eventually increasing the aging time to dry up the outer surface of the entrained sol [52].

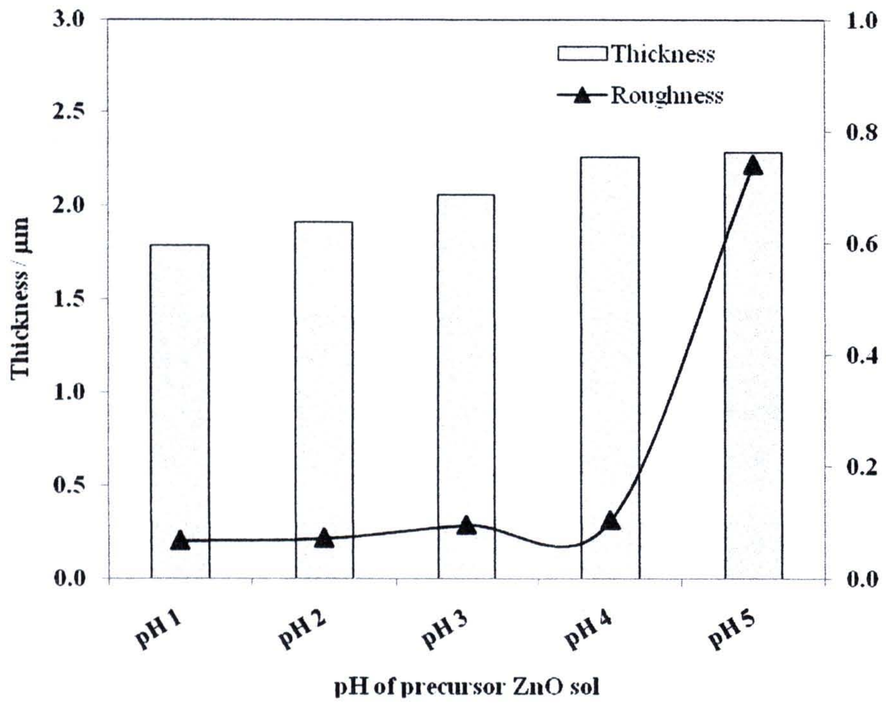

Figure 4.21 Film thickness and surface roughness as a function of pH of precursor ZnO sol

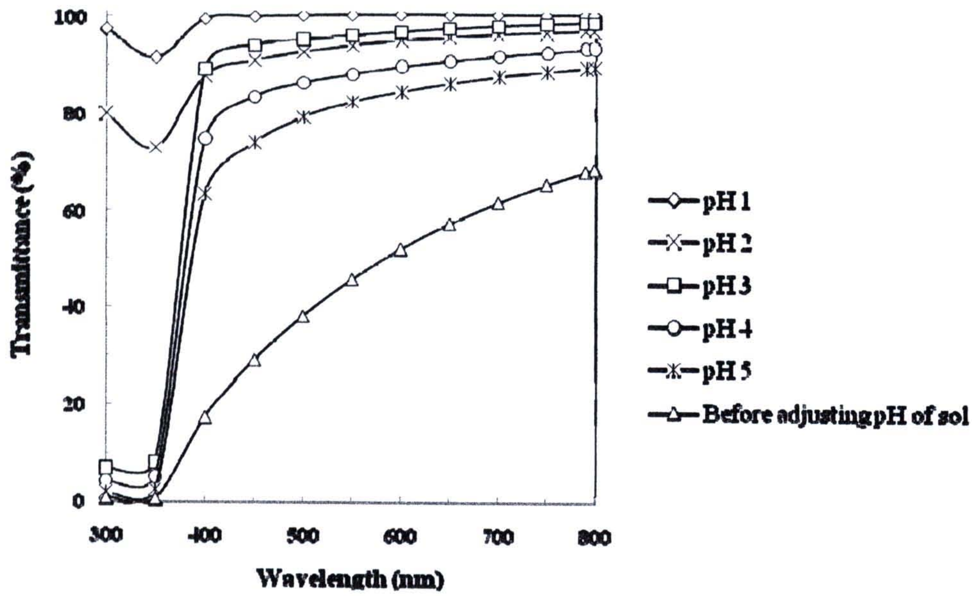

Figure 4.22 Optical transmittance spectra of ZnO embedded in PET film from different pH of precursor sol

Figure 4.22 shows the effect of pH of precursor ZnO sol on the optical properties of the ZnO embedded in PET film. Results showed that most the film have a transmittance over than 70 % in the visible range. Especially for the ZnO film as prepared by precursor ZnO sol at pH 1 exhibited an average transmittance in the visible range is above 99%. With the increase pH of sol, the transmittance of ZnO thin film in the visible range is gradually decreased. Nevertheless the pH of sol does not affect the strong absorption property of ZnO thin film in the ultraviolet range and the absorption edges of the samples all lay at ~370 nm.

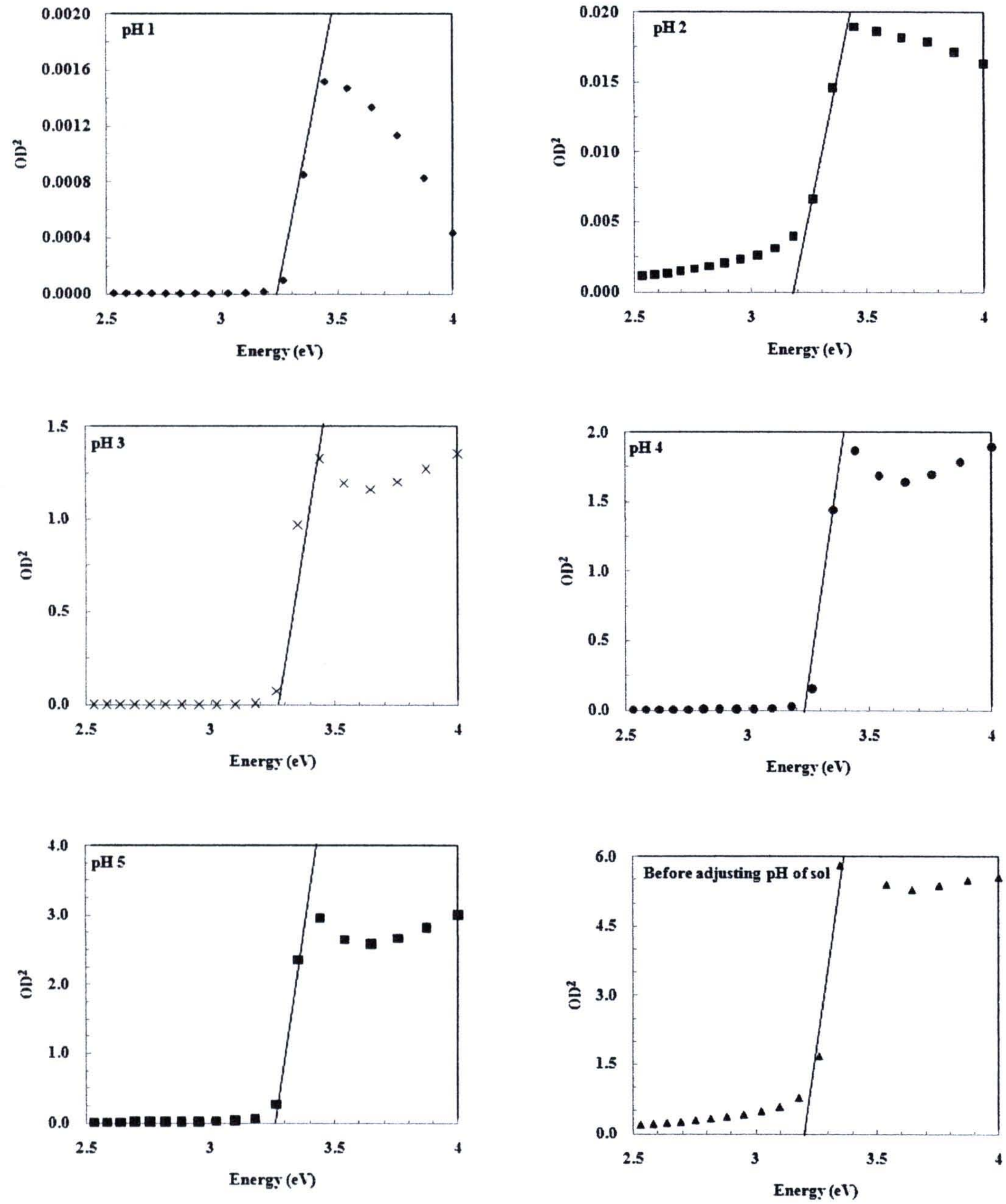

Figure 4.23 A plot of OD^2 vs energy for finding intercept on x axis that represents the gap width of ZnO embedded in PET film

The fundamental absorption corresponds to electron excitation from the valence band to the conduction band can be used to calculate the value of the optical band gap that relates to the characteristic of the material [53]. These relation evaluated by plot of the square of the optical density (OD, OD = log (100/T) as a function of $h\nu$ in Figure 4.23 gives the gap width for films with various pH of sol. The h is a Planck's constant as $6.620\times^{10-34}$ J·s. The number of carrier ν can be deduced from c/λ with c as a speed of light where λ is a wavelength of photon. Curves are limited at the high photon energies by the absorption of the substrate. The value of the gap width of all the samples were around 3.2-3.4 eV which is quite nearly the band gap energy of ZnO (3.37 eV). The evidence reveals that the surface of the film has ZnO filler on the surface. Wherein, the two major factors effect on the transmittance were surface roughness and grain size of the film. Therefore, the surface morphology of the high transparent ZnO embedded in PET film was observed by FESEM which was chosen the pH of the precursor ZnO sol of 1 and 2 due to their optical properties (see in Figure 4.22).

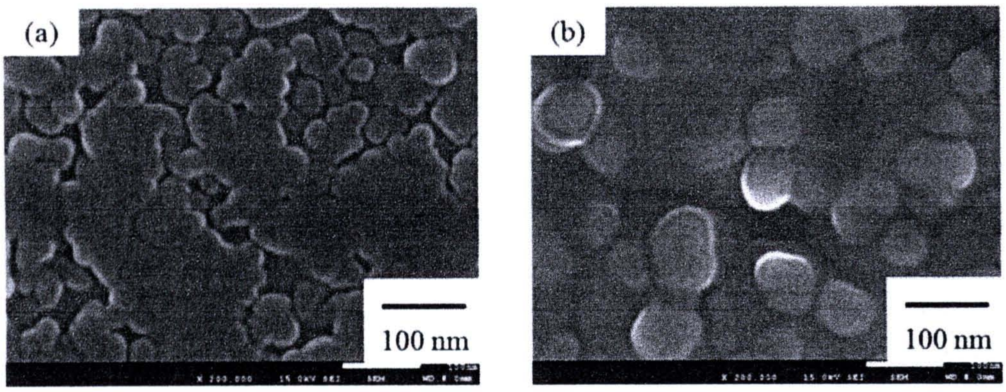

Figure 4.24 FE-SEM images of ZnO embedded in PET film as prepared at (a) pH = 1.0 and (b) pH = 2.0

Figure 4.24 shows the surface morphology images of ZnO embedded in PET film prepared by precursor of ZnO sol with pH 1 and pH 2. It was found that the grain size of the films depend on pH of the sol with the pH 1 estimated the average grain size about 20 nm and increased to 50 nm as the increased pH of sol to 2. The increased pH of sol also relates to the surface roughness of the film. Consequently, the optical transmittance of the film as the prepared with the higher pH of ZnO sol exhibited the decreased transmittance of the film at the larger grain size and higher surface roughness of the film. Base on our experiment, the morphology of ZnO thin film is determined mainly by the competition between the polycondensation of hydrolyzed zinc acetate and the zinc oligomers adsorbed by PET film. The large amount of H^+ ions in the low pH of sol inhibited hydrolysis and condensation process of the sol through polymerization of the metal-oxygen bonds leads to the smaller grain size of the film in low pH. This evidence tend to support the experimental of Houng et al., reported at higher pH accelerates the rate of hydrolysis and polycondensation that affects the highly branched metal-oxygen polymeric network resulted in a larger grain microstructure in the film [26]. On the other hand, the competitive of zinc oligomers adsorbed in the cavities of the PET film probably occurs randomly so the grain-boundary of the film is not so clear in both of the FE-SEM image of the film prepared with pH 1 and 2.

4.6.2 Investigation of the hydrophilic property of the ZnO embedded in PET film

The hydrophilic of the ZnO embedded in PET film was investigated by measuring the water contact angle. It's well known that the wettability of the surface depends on two main factors, i.e. surface roughness and UV light irraditation time were studied in these factors. Therefore, the surface roughness of the ZnO embedded in PET film observed by SPM was shown in Figure 4.25. It was found that the pH 1 of precursor of ZnO sol embedded in PET film showed the flattest surface among the film. The smaller size of ZnO oligomer adsorbed in the cavities of the PET film then it can be obtained in smaller particles embedded in the surface as shown in Figure 4.25(a). On the other hand the ZnO thin film from ZnO sol pH 2 exhibited the greater size of particle agglomerate on the surface (Figure 4.25(b)) due to the effect of pH of sol precursor. The decreased H^+

ions at the higher pH of sol probably affect the lower rate of polycondensation of the metal oxide as a result in the bigger particle growth on the film. Therefore, the higher surface roughness of the ZnO film from pH 1 gave the lower contact angle than the film as prepared by the ZnO sol-gel at pH 2. Result showed that the wettability of a surface may depends on their surface roughness. The relationship between the roughness surface and the hydrophilic property of the film was explained by Wenzel's model that described the water contact angle on rough and solid surfaces [19, 44, 47]. The model illustrates that the hydrophilic surface becomes more hydrophilic surface when the surface roughness enhances. The increased surface roughness also provides the highly hydrophobic in the case of hydrophobic surface. Miyauchi et al. reported that the water contact angle of the flat TiO_2 surface less than 90°, as with most inorganic substances [47]. Then, the surface of TiO_2 become more hydrophilic when roughness is provided that corresponded to Wenzel's model.

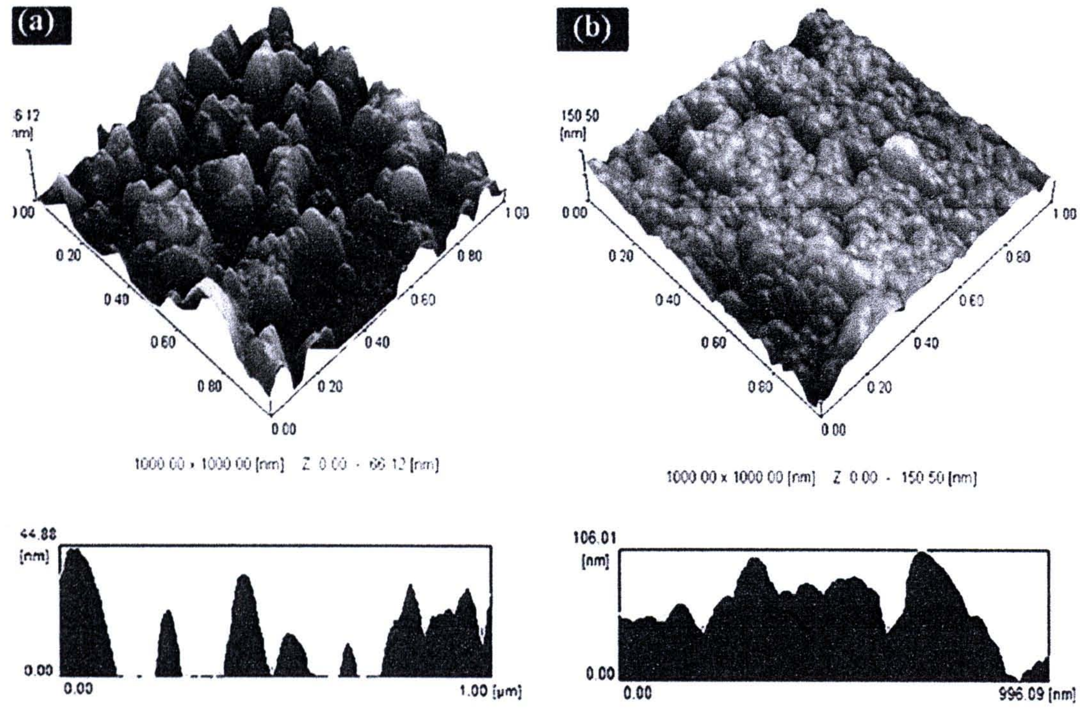

Figure 4.25 2D and 3D topographical (1µm×1µm) of the ZnO embedded in PET film prepared by the different pH of precursor of ZnO sol (a) pH 1 and (b) pH 2

In order to investigate the effect of the UV irradiation time on the hydrophilic property of the ZnO embedded in PET film, the film exposure to the light irradiation in the atmospheric air at different five areas. It can be seen from Figure 4.26 that the changeable water contact angle of the films after UV irradiation time.

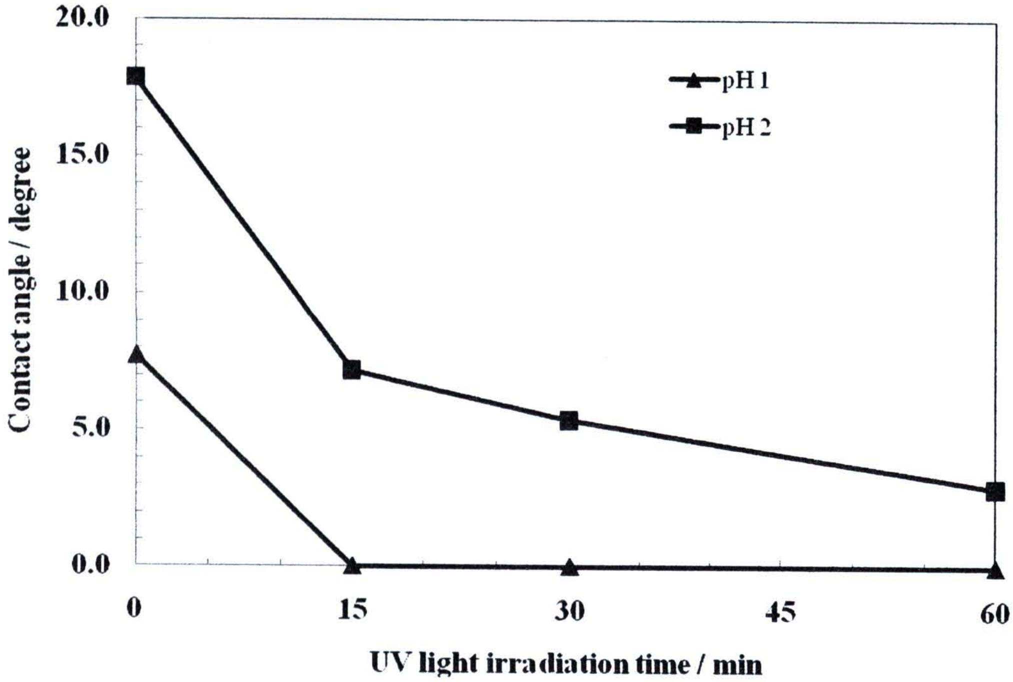

Figure 4.26 Water contact angle as induced by the UV light irradiation of the ZnO embedded in PET film as prepared by the various pH of precursor of ZnO sol

Prior to light illumination, the film as prepared by pH 1 and pH 2 of precursor of ZnO sol were water contact angles around 8° and 18°, respectively. Upon UV light illumination, the water contact angle for the both of the film from pH of ZnO precursor sol as 1 and 2, dramatically decreased to 0° and 7° after 15 min UV exposed time. In addition, after 30 min UV irradiation time, the films achieved again a low water contact angle values of 0 and 5 degree for the film as prepared at pH 1 and 2, respectively. However, the contact angle of zero still exhibited after the UV illumination of 15 to 60 min in the case of the pH 1 ZnO sol embedded in PET film. During the UV irradiation is attributed to structural changes at the surface. The electron and hole generated by ZnO under band gap illumination diffuse to the surface to react with lattice metal ions Zn^{2+} to form Zn^{2+} defective sites and the lattice oxygen resulting in the formation of surface oxygen vacancies, respectively. The oxygen vacancies are apparently favorable coordinate to water molecules, leading to the increasing water adsorption as a cause in the highly hydrophilic surface were formed. Based on results, the surface roughness of ZnO embedded in the PET film affects the wettability of the surface of the film. Even at longer irradiation time, pH 1 (rougher surface, low ZnO) produced lower contact angle compare to pH 2 (smooth surface, high ZnO). Hence, surface roughness provides more than defective sites (produced by UV irradiation) in ZnO in terms of wettability of the surface film. In addition at lower pH, produced lower concentration of OH^- which eventually formed to less a $Zn(OH)_2$ in the sol. To confirm these results, the quantity of ZnO embedding in polyelectrolyte film with prepared at pH 1 and 2, were analyzed by energy dispersive X-ray spectroscopic which present in Table 4.13 and 4.14, respectively. Results reveal that a lower pH of precursor sol could afford low content of ZnO in film due to adjusting the pH of the precursor sol by acetic acid. Therfore, the formation ZnO through sol-gel process at lower OH^- (low pH) to react with Zn^{2+} and then easily to form ZnO, it would be difficult. This result also supports the research work of Rani et al.. They studied the larger pH (6-11) on the growth of ZnO nanoparticles in zinc acetate solution. The sol having pH<7 could have insufficient OH^- that affects the growth of ZnO paricle as a cause lack of $Zn(OH)_2$ to become ZnO after calcinations [31]. Thus, the threshold of pH level may control sol-gel process in nanostructure to formation.

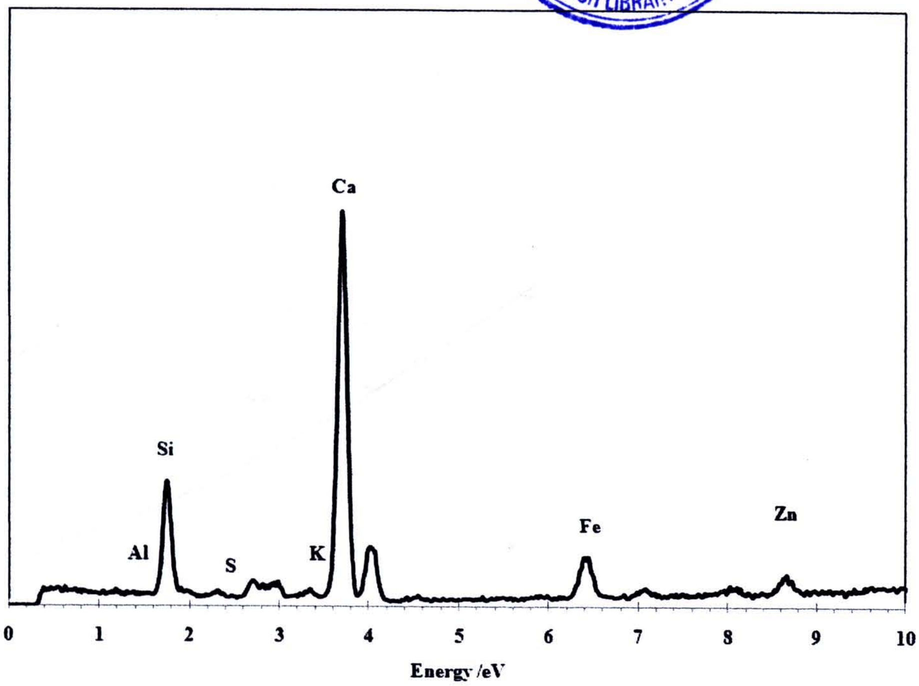

Figure 4.27 EDX analysis of ZnO film prepared by sol-gel precursor pH 1 at withdrawal speed 3 cm/min and calcination temperature of 500°C for 1 h

Table 4.13 Summary of the oxide compounds on the ZnO film (by sol-gel precursor pH 1 at withdrawal speed 3 cm/min and calcination temperature of 500°C for 1 h) observed by EDX

Oxide compound	Weight percent
Al_2O_3	2.63
SiO_2	85.40
SO_3	0.94
K_2O	0.31
CaO	10.51
Fe_2O_3	0.18
ZnO	0.03

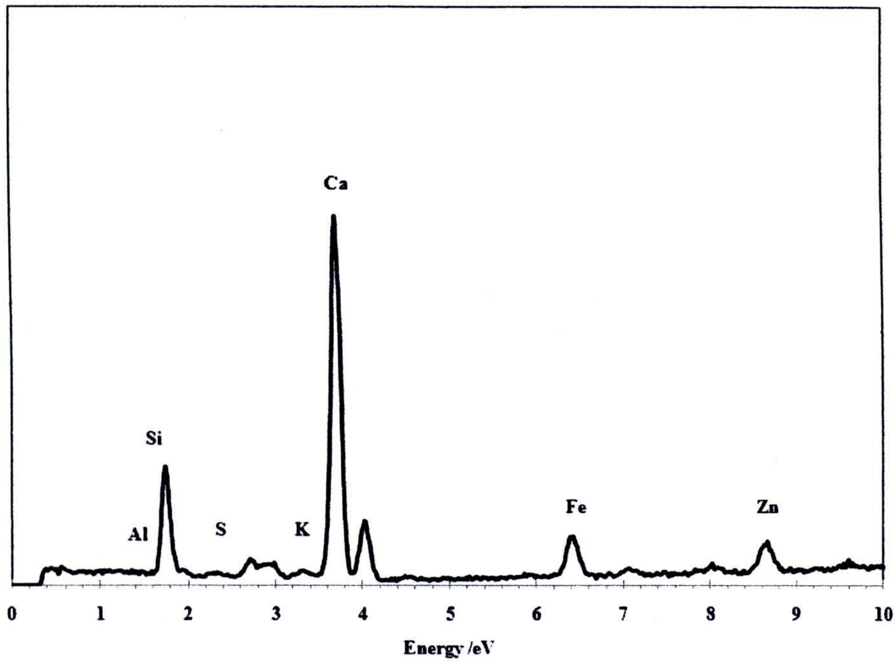

Figure 4.28 EDX analysis of ZnO film prepared by sol-gel precursor pH 2 at withdrawal speed 3 cm/min and calcination temperature of 500°C for 1 h

Table 4.14 Summary of the oxide compounds on the ZnO film (by sol-gel precursor pH 2 at withdrawal speed 3 cm/min and calcination temperature of 500°C for 1 h) observed by EDX

Oxide compound	Weight percent
Al_2O_3	2.40
SiO_2	85.63
SO_3	0.74
K_2O	0.30
CaO	10.70
Fe_2O_3	0.18
ZnO	0.05

As the results, these experiments suggest that transparent film of ZnO incorporated with polyelectrolyte film coated on glass substrate using layer-by-layer and dip coating technique should prepare by sol-gel which exhibit good photoinduced hydrophilic property in a short time (15 min). Although, this method would decompose polyelectrolyte film since the film prepared by sol-gel would be calcined at the high temperature of 500°C to formation ZnO in the film. In summary based on all experimental results conducted in this work, the hydrophilic property of the fabricated ZnO incorporated with polyelectrolyte films are attributed to their surface roughness, grain size, distribution and quantity of ZnO which are in turn affected by the number of coating layer (precipitation method), precursor concentration (suspension of ZnO in PAA) and pH of precursor solution (sol-gel method).